DENTAL MATERIALS 36 (2020) e365–e374

Available online at www.sciencedirect.com

ScienceDirect

journal homepage: www.intl.elsevierhealth.com/journals/dema

Microstructural, mechanical, and optical characterization of an experimental aging-resistant zirconia-toughened alumina (ZTA) composite

A.C.O. Lopes[a,*], P.G. Coelho[b,c,d], L. Witek[b], E.B. Benalcázar Jalkh[a,b], L.A. Gênova[e], K.N. Monteiro[f], P.F. Cesar[f], P.N. Lisboa-Filho[g], E.T.P Bergamo[a], I.S. Ramalho[a], T.M.B. Campos[h], E.A. Bonfante[a]

[a] Department of Prosthodontics and Periodontology, University of São Paulo – Bauru School of Dentistry, Bauru, SP, Brazil
[b] Department of Biomaterials and Biomimetics, New York University College of Dentistry, New York, NY, USA
[c] Hansjörg Wyss Department of Plastic Surgery, NYU Langone Medical Center, New York, NY, USA
[d] Mechanical and Aerospace Engineering, NYU Tandon School of Engineering, New York, NY, USA
[e] Institute of Research in Nuclear Energy, SP, Brazil
[f] Department of Biomaterials and Oral Biology, University of São Paulo, School of Dentistry, SP, Brazil
[g] Department of Physics, São Paulo State University, Bauru, SP, Brazil
[h] Physics Departament, Aeronautics Technological Institute (ITA), São José dos Campos, SP, Brazil

ARTICLE INFO

Keywords:
Composites
ZrO_2–Al_2O_3
Mechanical properties
Optical properties

ABSTRACT

Objective. To evaluate the effect of aging on the microstructural, mechanical, and optical properties of an experimental zirconia-toughened alumina composite with 80%Al_2O_3 and 20%ZrO_2 (ZTA Zpex) compared to a translucent zirconia (Zpex) and Alumina.

Methods. Disc-shaped specimens were obtained by uniaxial and isostatic pressing the synthesized powders (n = 70/material). After sintering and polishing, half of the specimens underwent aging (20 h, 134 °C, 2.2 bar). Crystalline content and microstructure were evaluated using X-ray diffraction and scanning electron microscopy, respectively. Specimens underwent biaxial flexural strength testing to determine the characteristic stress, Weibull modulus, and reliability. Translucency parameter (TP) and Contrast ratio (CR) were calculated to characterize optical properties.

Results. ZTA Zpex demonstrated a compact surface with a uniform dispersion of zirconia particles within the alumina matrix, and typical alumina and zirconia crystalline content. ZTA Zpex and alumina exhibited higher CR and lower TP than Zpex. ZTA Zpex and Zpex showed significantly higher characteristic stress relative to alumina. While aging did not affect optical and mechanical properties of ZTA Zpex and alumina, Zpex demonstrated a significant increase in translucency, as well as a in characteristic stress. Alumina reliability was significantly lower than others at 300 MPa, ZTA Zpex and Zpex reliability decreased at 800 MPa, except for aged Zpex.

* *Corresponding author at*: Adolfo Coelho de Oliveira Lopes, Department of Prosthodontics and Periodontology, University of São Paulo, Bauru School of Dentistry, Al. Octávio Pinheiro Brisola 9-75, Bauru, SP, Brazil.
E-mail address: acol_sp@hotmail.com (A.C.O. Lopes).
https://doi.org/10.1016/j.dental.2020.08.010

Significance. While aging did not affect the mechanical nor the optical properties of ZTA Zpex and alumina, it did alter both properties of Zpex. The results encourage further investigations to engineer ZTA as a framework material for long span fixed dental prostheses specially where darkened substrates, such as titanium implant abutments or endodontically treated teeth, demand masking.

1. Introduction

Yttria-stabilized tetragonal zirconia polycrystals (Y-TZP) were introduced as an alternative to metal–ceramic prostheses for esthetic dental rehabilitations and have received remarkable popularity because of its excellent properties such as improved aesthetic, biological acceptance, chemical durability and outstanding mechanical properties [1]. Zirconia occurs naturally in three allotropic crystalline structures, which are stable according to a given temperature range: monoclinic (m; room temperature up to 1170 °C), tetragonal (t; 1170 °C until 2370 °C), and cubic (c; 2370 °C up to the melting point, 2710 °C) [1–3].

The excellent mechanical properties of zirconia systems are related to a phenomenon known as transformation toughening mechanism, which can be explained by the ability of tetragonal zirconia grains to undergo a stress-mediated phase transformation to the monoclinic phase. This phenomenon is responsible for the highest fracture toughness presented by Y-TZP related to all-ceramic systems currently used in dentistry by consistently evoking the R-curve behavior, i.e. the increase of fracture toughness during crack growth [4]. Despite the evident advantage of such mechanism, this material undergoes spontaneous tetragonal to monoclinic phase transformation at low-temperature in the presence of water, a phenomenon known as low-temperature degradation (LTD) [1–3], which may eventually impair the probability of survival and mechanical properties of prosthetic rehabilitations in the long-term.

Several efforts have been made in the ceramic field to increase the resistance to LTD of zirconia ceramics by various techniques [5]. A possible alternative to enhance the hydrothermal stability of the tetragonal phase of Y-TZP is the addition of alumina to inhibit the propagation of phase transformation into the material. Zirconia-toughened alumina (ZTA) contains zirconia particles dispersed as a second phase in an alumina matrix, bringing together the beneficial features of both materials [6], which contributes to the stability of zirconia [6,7]. It has been established that LTD phenomenon occurs by a nucleation and growth process; where the transformation occurs on isolated grains on the surface and propagates from grain to grain. Therefore, previous literature findings have shown that alumina limits the interconnectivity of zirconia grains within the matrix, restricting phase transformation and decreasing LTD phenomenon [8,9].

The maximum zirconia fraction to limit the propagation of transformation is associated to the interconnectivity of the zirconia phase, namely the percolation threshold [10]. Zirconia grains interconnectivity within the alumina matrix have been investigated in attempt to establish the proportion of tetragonal zirconia that may limit LTD process. Composites with a proportion between 15% and 30% of zirconia in an alumina matrix has demonstrated promising mechanical results, with a significant increase in strength after aging, which makes it a material candidate for application in areas that requires high mechanical resistance [11]. Nonetheless, the opacity of ZTA composites may pose a challenge to dental technicians, demanding elevated skills to achieve esthetic porcelain veneering, justifying further innovations [12,13].

Therefore, in an attempt to reduce the risk for long-term complications due to the metastability of Y-TZP, this study aims to evaluate the microstructure, optical and mechanical properties of an experimental zirconia-toughened alumina (ZTA) composite fabricated with 80% Al_2O_3 and 20% translucent Y-TZP and to compare them to their isolated counterparts (translucent Y-TZP or Al_2O_3) before and after aging. The postulated null hypothesis was that the aging protocol would not affect the microstructural, mechanical, and optical properties of ZTA Zpex 80/20 composite.

2. Material and methods

2.1. *Specimen preparation*

A total of two hundred and ten disc-shaped specimens were fabricated from two experimental ceramics (n = 70/material), as follows: (i) ZTA Zpex 80/20: zirconia-toughened alumina (ZTA) composite (80%Al_2O_3/20%Zpex), (ii) Zpex: translucent Y-TZP zirconia and (iii) Alumina (α-high-purity Al_2O_3).

A translucent zirconia (Y-TZP Zpex, Tosoh Corp., Japan) and high-purity alumina (α-Al2O3, Baikalox Regular CR10, Baikowski) powders were used to produce the specimens of Alumina, Zpex and ZTA Zpex 80/20 groups. For composite synthesis, the ceramic powders were mingled in ethanol suspensions, then blended and homogenized in a friction mill for 4 h with high purity alumina balls. A rotary evaporator (801, Fisaton, SP, Brazil) was used to dry the slurry, and the obtained powder was manually granulated with the aid of an alumina Mortar and Pestle set and sieved with a 0.475-mm (No. 40) sieve. The composition characteristics and the theoretical density values were calculated based on the density of alumina (3.986 g/cm^3) and zirconia (6.10 g/cm^3).

Subsequently, the ZTA Zpex 80/20, Apex, and Alumina powders were uniaxially pressed for 30 s at 1148 Kgf. A tungsten carbide cylindrical matrix (9-cm height and 5-cm diameter) with a retractable base and an internal piston for disc pressing, and a 15-mm diameter internal hole, was used to achieve 1.8-mm thickness disc-shaped green body samples. Then, they were double enveloped in a vacuum sealer and subjected to

isostatic pressing (National Forge, Pennsylvania, USA) at room temperature.

The sintering of the green body samples was performed at 1600 °C for 1 h in a Zyrcomat (Vita Zahnfabrink, Bad Säckingen, Germany) furnace with a heating and cooling rate of 4 °C per minute. After sintering, both disc sides were polished by using a series of abrasive diamond disks (#220, 120, 90, 40, 25, 9, 6 and 1 μm, ALLIED High Tech Products, California, USA) in a semi-automatic polishing machine (Automet 2000, Buehler, Illinois, USA) with diamond suspensions up to 1 μm until the final dimension of 12 mm × 1 mm (diameter × thickness) had been achieved (ISO 6872:2015). The final thickness of each disc was assessed with a digital caliper (Starrett 799A-6/150 Digital Caliper, Athol, MA, USA).

2.2. Simulated LTD aging

The aging protocol was performed in autoclave (Vitale Class CD 12L, PR, Brazil) for 20 h in water vapor at 134 °C and 2.2 bar to induce tetragonal-to-monoclinic phase transformation, according to ISO13356:2015 (n = 30/group) [14,15].

2.3. X-ray diffraction (XRD)

X-ray diffraction (XRD) (X'pert Power PANalytical, Netherlands) was used to analyze the crystalline content and progression of the t-m transformation due to accelerated aging. The scanning was performed on the Bragg θ-2θ geometry, equipped with a graphite monochromator and Cu Kα radiation (λ = 1.5406 Å), operating at a voltage of 40 kV and a current emission of 40 mA. The XRD analysis was performed using step scan with a step size of 0.02° and between 20 and 70° (2θ).

The monoclinic phase content of surfaces was calculated using the Toraya and Yoshimura method. [16]

$$X_m = \frac{[I_m(-111) + I_m(111)]}{[I_m(-111) + I_m(111) + I_t(101)]}$$

$$V_m = 1.311\,X_m / (1 + 0.311\,X_m)$$

where X_m, the integrated intensity ratio, is defined by the I_m (−111) and I_m (111) that represent the monoclinic peaks intensity (2θ = 28° and 2θ = 31.2°, respectively) and I_t (101) that indicates the intensity of the tetragonal peak (2θ = 30°); V_m represents the monoclinic volumetric content.

The residual stress was also determined by means of XRD analysis (Empyrean, PANalytical, The Netherlands), with the same equipment described above, where the scanning was performed from 90 to 100° setting 10 s per scan step [17]. The evaluation of the residual stress by XRD is based on measuring the change of the interplanar spacing of crystal lattice. Thus, the measurement of the residual stress using XRD consisted of varying the beam penetration by changing the angle of incidence (Psi) to analyze the displacement of the peak as a function of depth. Hence, several spectra were obtained varying the Psi for the different ceramic materials. The peak displacement was analyzed at 95°, which was determined considering the value of 2θ corresponding to the center of the peak. With the values of the peak position as a function of the incidence Psi angle, the planar distance (d) was calculated. Thus, correlating the variation of d of different Psi enables residual stress (σ_ϕ) calculation. This equation relates the σ_ϕ as a function of the square sine of the incidence angle – Sin^2(Psi) [18]:

$$\sigma\phi = \frac{d\psi - d0}{d0}\,\frac{E}{1+\upsilon}\,\frac{1}{sin^2\,\psi}$$

where ν is the Poison ratio and E the elastic modulus.

2.4. Scanning electron microscope (SEM)

To characterize the topography and microstructure of the experimental materials, high-resolution scanning electron microscopy by (FEG-SEM MIRA3 TESCAN, Czech Republic) analyses (Magellan 400L, FEI Company, Brno, Czech Republic) were performed, with a secondary electron (SE) detector under magnification of 20,000×.

2.5. Biaxial flexural strength and fractographic analysis

Thirty specimens for each group and condition (immediate and aged) were subjected to biaxial flexural strength test using a piston-on-three balls device (BFST), according to ISO 6872:2015 guidelines and demonstrated in previous studies [19–21]. BFST was carried out in an ElectroPulsTM E3000 Linear-Torsion (Instron, Norwood, Massachusetts, EUA) equipment at a crosshead speed of 0.5 mm/min, until failure. Fracture load (N) data were collected and submitted to specific equations (ISO 6872:2015) to obtain the flexural strength (MPa), as follows:

$$\sigma = -0.2387.^{p(X-Y)}/_{b^2}$$

where σ is the maximum tensile stress (MPa), p is the total load to fracture (N), b is the thickness at fracture origin (mm), and X and Y are calculated according to:

$$X = (1+\upsilon)\,ln(r2/r3)^2 + [(1-\upsilon)/2](r2/r3)^2$$

$$Y = (1+\upsilon)\,[1 + ln\left(\frac{r1}{r3}\right)^2] + (1-\upsilon)(r1/r3)^2$$

where v is Poisson's ratio (=0.26), r_1 is the radius of support circle, r_2 the radius of loaded area, r_3 the radius of specimen, all of these expressed in millimeters.

Fractography analysis was used to study the characteristics of the fractured surface. Different modes of failure produce specific features on the surface, allowing a forensic analysis to determine the root cause of the fracture. Fractured samples were first inspected in polarized light microscope (Axiom V16, Zeiss, Germany) using automated Z-stack imaging that combined different depths (every 70 μm) of the fracture plane into one image (ZEN software, Zeiss) with improved depth of focus for detection of failure origin and direction of crack propagation. To depict fractographic marks typical of brittle failure of shaped ceramic samples, SEM was used to confirm initial inspection and to document mirror, hackles, and compression curl areas.

2.6. Optical properties

For optical properties analysis, the contrast ratio (CR) and translucency parameter (TP) by color difference (ΔE) measurements were determined using parameters obtained by reflectance tests performed with a bench top spectrophotometer (CM 3700d Konica Minolta, Tokyo, Japan). The specimens were placed on a black (b) and white (w) background for the measurement of reflectance values and CIEL*a*b* color coordinates with a wavelength of 400–700 nm (within visible light range) (n = 10/material) [22].

Prior to testing, the spectrophotometer was calibrated according to manufacturer's instructions. Two accessories were used for calibration: a white calibration plate CM-A90 (Konica Minolta) and a black calibration box CM-A94 (Konica Minolta). The black box calibrates the absolute zero, where the accessory absorbs the light emitted during the test, whereas the white calibration plate is used to set the equipment in the ideal regulation. For each device, three beams of light were produced with an interval of 10 s; first, the calibration was performed using the accessory of the white calibration and then with the black calibration. The information measured at the time of calibration is sent to the equipment software (OnColor software, CyberChrome, Beech Island, SC, USA), which then allows the equipment to perform the test.

The specimens were positioned on the background card (white or black) with glycerol to attenuate the reflective effect of the presence of air. The spectrophotometer was equipped with an integration sphere (150 mm diameter and coated with $BaSO_4$) and a light source (xenon arc lamp). The light emitted by the light source diffuses in the sphere and evenly illuminates the surface of the specimen, passing by the illumination door. By capturing the image of the specimen, the spectral sensor, where the light is divided by the wavelength of 360–740 nm at 10 nm intervals, is able to detect its color. Segments of silicon matrix convert light into electric current, which passes to circuits to convert it into digital signals; the data were obtained using the equipment software.

The opacity of the specimen in terms of CR (CR = Yb/Yw) is defined as the ratio of reflectance of the material on the black background to the reflectance of the same material on a white background:

$$CR = Yb/Yw$$

Masking ability (translucency parameter – TP) of the materials was determined by measuring the ΔE over white and black backgrounds, using the following formula:

$$\Delta E = \left[\left(L_b^* - L_w^*\right)^2 + \left(a_b^* - a_w^*\right)^2 + \left(b_b^* - b_w^*\right)^2\right]^{1/2}$$

where the L* coordinate represents the lightness of an object. The a∗ coordinate corresponds to the chromaticity on the red/green axis and b∗ on the yellow/blue axis. The subscripts b* (black) and w* (white) indicate background color.

A total of 10 specimens for each ceramic group (immediate and aged) were used for the optical tests.

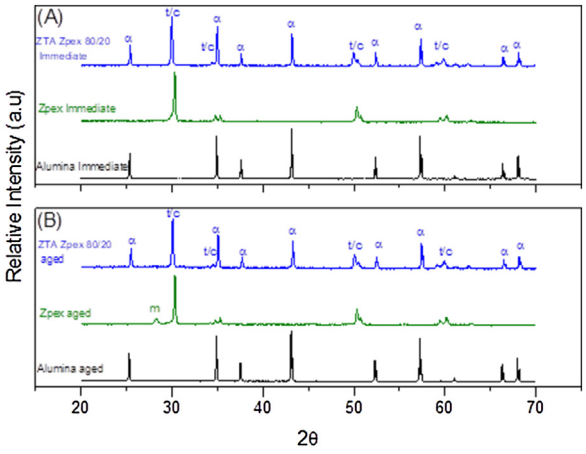

Fig. 1 – XRD patterns of the experimental materials before (A) and after aging (B), where the increase in the monoclinic peak (2θ = 28° and 2θ = 31.2°) for the Zpex group relative to ZTA composite is demonstrated.

2.7. Statistical analysis

Data from optical characterization were tabulated and subjected to descriptive analysis, normality and homoscedasticity test. Data were statistically evaluated through repeated-measures analysis of variance following post-hoc comparisons by Tukey test, with significance level set at $p < 0.05$. Data are presented as a function of estimated mean values with the corresponding 95% confidence interval (CI). All analyses were performed using SPSS (IBM SPSS 23, IBM Corp., Armonk, NY).

The flexural strength values were subjected to Weibull 2-parameter analysis using Weibull ++ software (Synthesis 9, Reliasoft, Tucson, AZ, USA). A use level probability Weibull was presented to determine probability of failure as a function of stress, and a Weibull 2-parameter contour plot (Weibull modulus [m] vs characteristic stress [η]) was used (95% confidence intervals) to determine differences between groups. Non-overlap of contour plots indicates a significant difference between them. Additionally, the probability of survival (reliability) at 300, 500, and 800 MPa flexural strength values was calculated for each group to evaluate their potential as restorative frameworks as detailed in the ISO 6872:2015.

3. Results

3.1. X-ray diffraction

XRD spectra of the materials are depicted in Fig. 1. Typical alumina and zirconia peaks can be identified, and the monoclinic crystalline content quantified. While the monoclinic content was stable after artificial aging in ZTA Zpex 80/20 composite and alumina, Zpex group showed a notable increase of monoclinic peak (2θ = 28° and 2θ = 31.2°) after aging protocol. The quantification analyses depicted approximately 26% monoclinic phase for Zpex relative to less than 2% for ZTA Zpex 80/20 after aging.

Fig. 2 shows the diffractogram of immediate and aged Zpex for different incidence angle (Psi), ranging from 0.000 to 0.400.

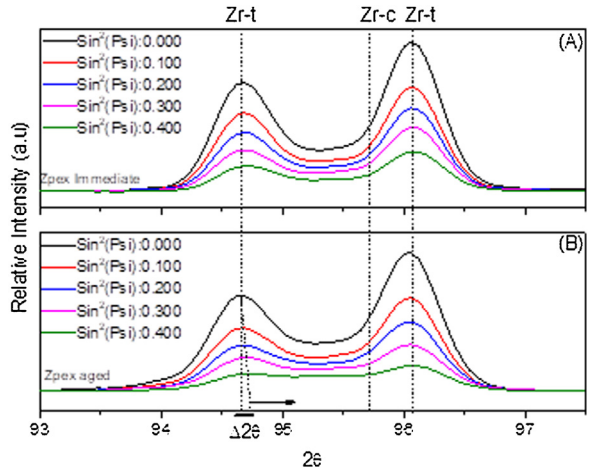

Fig. 2 – X-ray diffractograms of the immediate (A) and aged Zpex (B) samples for different incidence angle (Psi), ranging from 0.000 to 0.400, where the scanning was performed on the Bragg 2θ ranging from 90 to 100°.

The spectra depict the tetragonal zirconia peak at 94.5° and an overlap of tetragonal and cubic zirconia peaks at 96°. Immediate Zpex at the 94.5° peak had no displacement as a function of Psi, whereas aged Zpex presented a small shift of Psi. For aged Zpex, the higher the Psi, the larger the shift. As beam penetration is inversely proportional to Psi, more compressive stresses as a consequence of degradation process and volumetric increase of grains caused by phase transformation were present at the external surface of the disc. In addition, the calculated residual stress for aged Zpex, based on the elastic strain, which can be measured from the varying interplanar distances, and the elastic modulus of the material, was −464 ± 58 MPa. All other materials did not present any detectable residual stresses and were not included in the current analysis.

3.2. *Scanning electron microscopy*

SEM micrographs demonstrated morphological features of a fully crystalline matrix with a dense surface for Zpex, ZTA Zpex 80/20 and Alumina. Few microstructural intergranular flaws were found through the ceramic surface, which were related to the processing of the ceramic material (Fig. 3). The density values for ZTA Zpex 80/20 and alumina were 43,733 g/mL and 3989 g/mL, respectively, with approximately 98 % theoretical density, and for Zpex was 60,655 g/mL with 99% theoretical density.

While artificial aging did not influence the microstructure of ZTA Zpex 80/20 composite and alumina, Zpex group demonstrated a volumetric grain increase that provided a more compact surface (Fig. 3).

3.3. *Biaxial flexural strength and probability of survival predictions*

Table 1 shows the results of Weibull statistical analysis, with respective upper and lower 95% confidence bounds. The use level probability Weibull plot presented in Fig. 4A shows the failure distribution of samples as a function of stress. The calculated Weibull modulus (m) and characteristic stress (MPa), which indicates the stress in which 63.2% of the specimens may fail, are depicted in the contour plot (Fig. 4B). Significant differences were identified considering the non-overlap of the contours. Regarding the comparison between materials, while aged Zpex demonstrated the highest characteristic stress values; Alumina (immediate and aged) depicted the lowest values. ZTA Zpex 80/20 (immediate and aged) presented intermediated values, statistically similar to immediate Zpex. While the aging protocol did not influence the Weibull modulus and characteristic stress of ZTA Zpex 80/20 and Alumina, Zpex presented a statistically significant increase in characteristic stress.

The reliability at 300, 500 and 800 MPa with the corresponding 95% confidence interval is shown in Table 2. At 300 MPa, Zpex and ZTA Zpex 80/20 showed higher reliability (above 80%) relative to Alumina (immediate and aged), without significant difference between them. An increase in stress to 500 MPa did not significantly affect the reliability for ZTA Zpex 80/20 and Zpex groups, however Alumina groups demonstrated a significant decrease in reliability. At 800 MPa, all groups significantly decreased the reliability, except for aged Zpex. Aging did not affect the reliability values of the ZTA Zpex 80/20 composite and Alumina, whereas increased reliability was observed for aged Zpex.

All ceramic materials had similar fracture patterns. The defect that initiated the fracture event originated on the surface subjected to tensile stress during the flexural strength test. There were no critical defects in the corner area of the fracture surface. SEM images showed marks such as compression curl (CC) opposite to the failure origin, hackle lines (H) indicating the direction of crack propagation and fracture onset (arrow) (Fig. 5).

3.4. *Optical properties*

ZTA Zpex 80/20 and Alumina demonstrated statistically higher contrast ratio (CR) values compared to Zpex, for both conditions (immediate and aged, all $p < 0.002$). While aging protocol did not affect the opacity values of ZTA Zpex 80/20 ($p = 0.945$) and Alumina ($p = 0.277$), Zpex depicted a significant decrease in opacity values ($p < 0.001$).

Regarding the translucency parameter (TP), ZTA Zpex 80/20 presented a statistically significant lower ΔE in comparison to Zpex and Alumina for both conditions (immediate and aged) ($p < 0.001$). While aging protocol did not affect the ΔE values of ZTA Zpex 80/20 ($p = 0.767$) and Alumina ($p = 0.283$), Zpex showed a significant increase in ΔE values ($p < 0.001$) (Table 3).

4. Discussion

This study aimed to evaluate the effect of aging on the microstructure, optical and mechanical properties of an experimental zirconia-toughened alumina (ZTA) composite with 80%Al_2O_3 and 20%translucent Y-TZP (ZTA Zpex 80/20), compared to its isolated counterparts, alumina (Al_2O_3) and translucent Y-TZP (Zpex). ZTA Zpex 80/20, designed for restorative purposes, demonstrated a dense microstructure

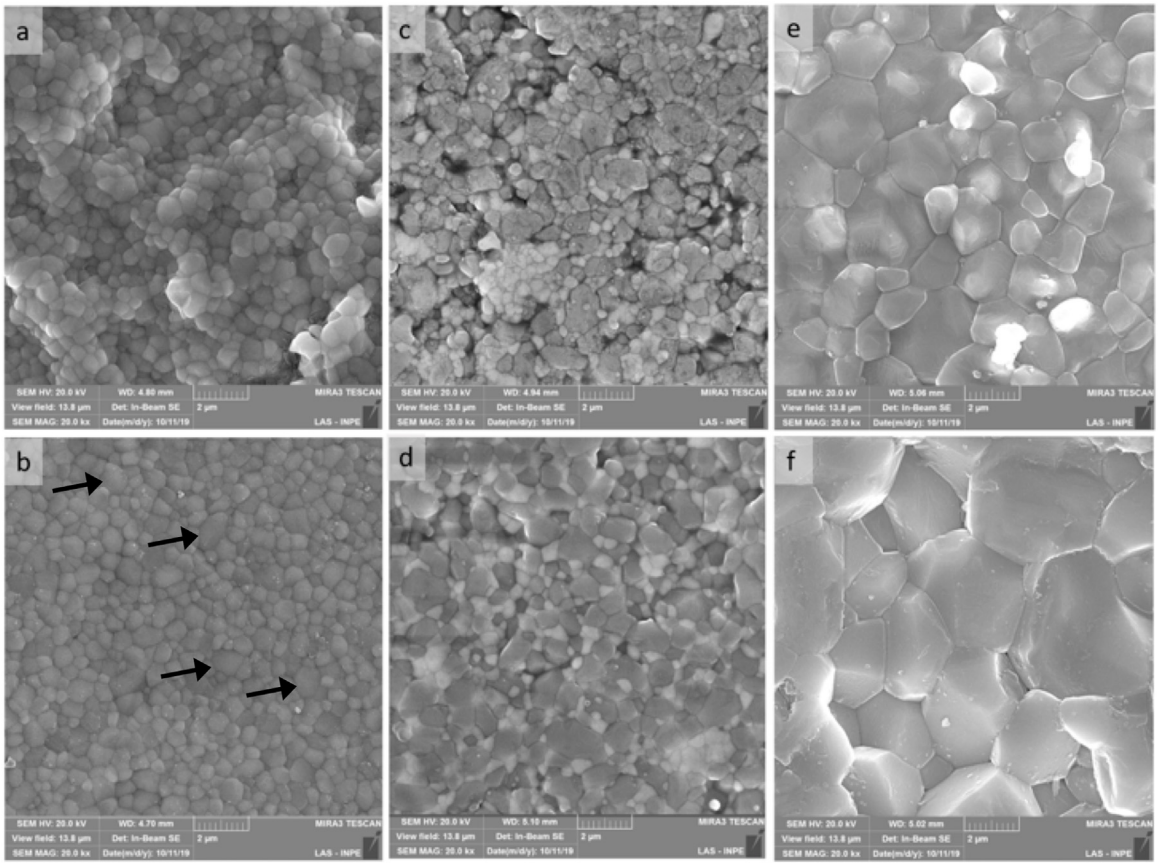

Fig. 3 – SEM micrographs of Zpex immediate surface a) and after aging protocol b). ZTA Zpex 80/20 immediate c) and aged d). Alumina immediate e) and after aging f). Images demonstrate the microstructural arrangement and final density obtained for Zpex, ZTA Zpex and Alumina. The arrows show the volumetric increase of grains caused by phase transformation.

Table 1 – Characteristic stress (η) and Weibull modulus (m) with their respective upper and lower 95% confidence bounds for immediate and aged groups.

	Zpex		ZTA Zpex 80/20		Alumina	
	Immediate	Aged	Immediate	Aged	Immediate	Aged
Upper	891.01	1384.14	950.25	975.32	434.61	504.63
Characteristic stress (MPa)	**860.31**^{B}	**1308.99**^{A}	**860.38**^{B}	**881.81**^{B}	**407.35**^{C}	**469.57**^{C}
Lower	830.59	1237.92	778.97	797.26	381.8	436.96
Upper	14.08	9.01	5.03	4.96	6.13	5.57
Weibull modulus (m)	**10.81**^{A}	**6.75**^{AB}	**3.8**^{C}	**3.77**^{C}	**4.9**^{BC}	**4.41**^{B}
Lower	8.3	5.06	2.88	2.86	3.92	3.5

Different letters indicate significant differences between groups.

and homogeneous distribution of zirconia particles within the alumina matrix. Such polycrystalline composite exhibited encouraging results concerning optical and mechanical properties, which remained stable after artificial aging. Therefore, the null hypothesis that the aging protocol would not affect the optical and mechanical properties of ZTA Zpex 80/20 composite was accepted.

Polycrystalline ceramic composites were introduced as an attempt to overcome the hydrothermal instability of Y-TZP, which occurs due its metastability and tetragonal (t) to monoclinic (m) phase transformation at low temperature, known as low temperature degradation (LTD) [1–3]. Such phenomenon can eventually compromise the mechanical properties and reliability of prosthetic treatments in the long-term [4]. The rationale behind the continuous development of ZTA composites is to effectively bring out the favorable properties of alumina and novel zirconia systems to enhance the ceramic properties, in which the optical properties and mechanical strength and toughness may be improved compared to alumina along with a better stability relative to the occurrence of LTD compared to Y-TZP [14,23–25]. Moreover, the proposed weight ratio of 20% zirconia particles uniformly disperse in 80% alumina matrix was based on previous investigations in composites targeted for Orthopedics [11,26,27]. Literature

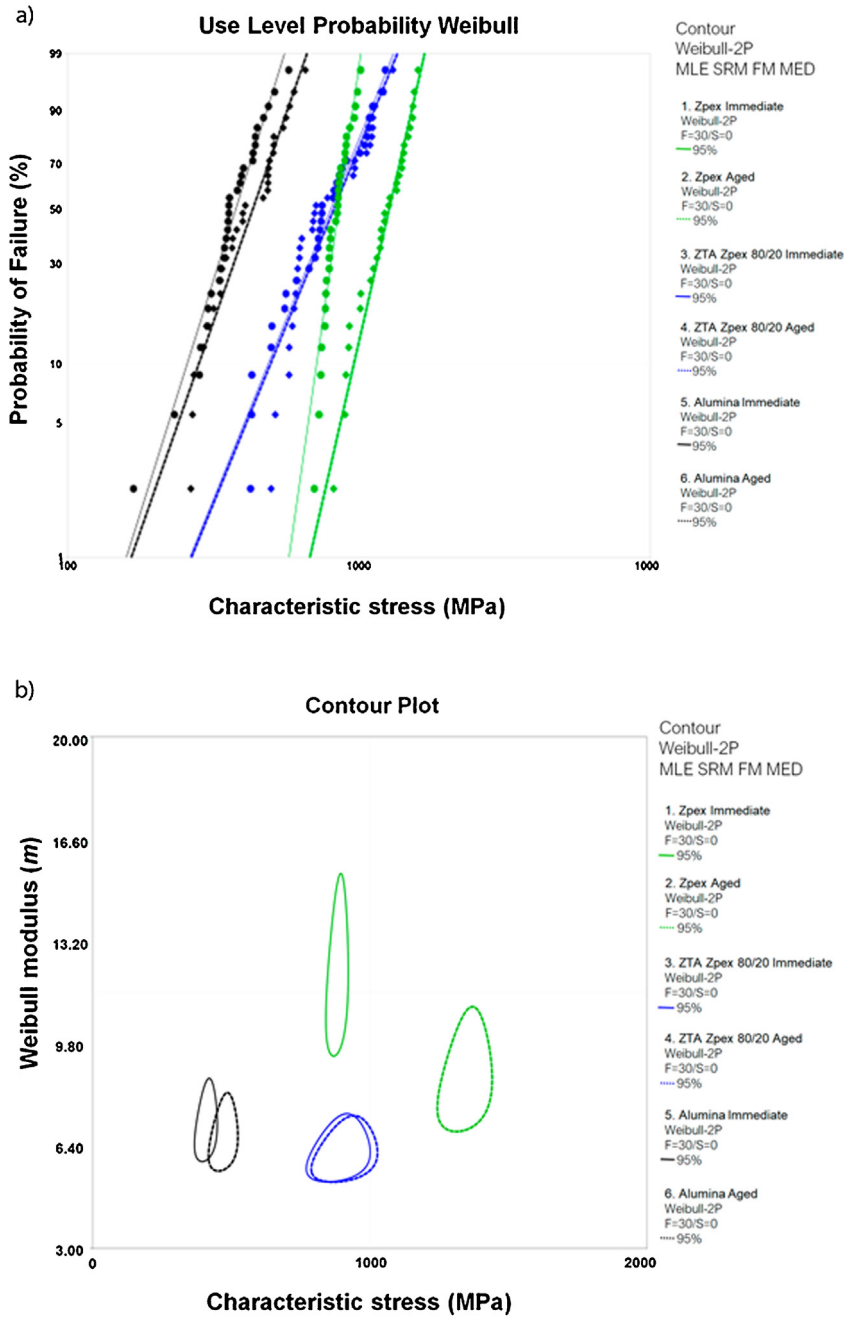

Fig. 4 – A) Use level probability Weibull shows sample failure distribution as a function of stress. B) Contour plot showing "*m*" as an indicator of reliability (Weibull modulus) vs. characteristic stress (η), which indicates the stress in which 63.2% of the specimens of each group may fail. The overlap between groups indicates they are homogeneous.

findings have shown excellent results regarding the LTD resistance of ZTA composites synthesized with 5–30 or 40% of Y-TZP [28,29], emphasizing the proportional improvement of composites mechanical properties with increasing percentage of zirconia in the composition. Also, composite with 15 and 30% of zirconia showed increased aging resistance with satisfactory performance for their application in areas of high functional demand [11].

The specimens were subjected to an aging process in an autoclave to simulate LTD [30], since the t-m phase transformation is dependent on temperature and accelerated by the presence of water [14,20,31]. The ISO 13356:2015 for Ceramic materials based on Y-TZP for implant surgery suggests that five hours of autoclave aging at 134 °C and 2.2 bar corresponds to approximately 4 years in vivo. The current study protocol, 20 h, has been chosen to promote an extensive t–m phase transformation, previously reported to range from 55% to 80% m-phase content [21,30,32], allowing a meaningful investigation of the susceptibility to degradation and the potential changes in optical, strength or reliability properties of the material. Accordingly, while experimental ZTA Zpex 80/20 exhibited a significant aging-resistant behavior through the

Table 2 – Calculated reliability at a set stress of 300, 500 and 800 MPa.

		Zpex		ZTA Zpex 80/20		Alumina	
		Immediate	Aged	Immediate	Aged	Immediate	Aged
300 MPa	Upper	1	1	1	1	0.88	0.93
	Reliability	$\mathbf{1}^{aA}$	$\mathbf{1}^{aA}$	$\mathbf{0.98}^{aA}$	$\mathbf{0.98}^{aA}$	$\mathbf{0.8}^{bA}$	$\mathbf{0.87}^{bA}$
	Lower	1	1	0.94	0.94	0.68	0.77
500 MPa	Upper	1	1	0.94	0.95	0.14	0.38
	Reliability	$\mathbf{1}^{aA}$	$\mathbf{1}^{aA}$	$\mathbf{0.88}^{bA}$	$\mathbf{0.89}^{bA}$	$\mathbf{0.07}^{dB}$	$\mathbf{0.27}^{cB}$
	Lower	0.98	0.99	0.76	0.77	0.02	0.17
800 MPa	Upper	0.76	0.99	0.6	0.64	0	0
	Reliability	$\mathbf{0.63}^{bB}$	$\mathbf{0.96}^{aA}$	$\mathbf{0.47}^{bB}$	$\mathbf{0.5}^{bB}$	$\mathbf{0}^{cC}$	$\mathbf{0}^{cC}$
	Lower	0.47	0.89	0.32	0.35	0	0

Different lowercase letters mean statistical difference between groups at the same stress level.
Different uppercase letters mean statistical difference between stress levels.

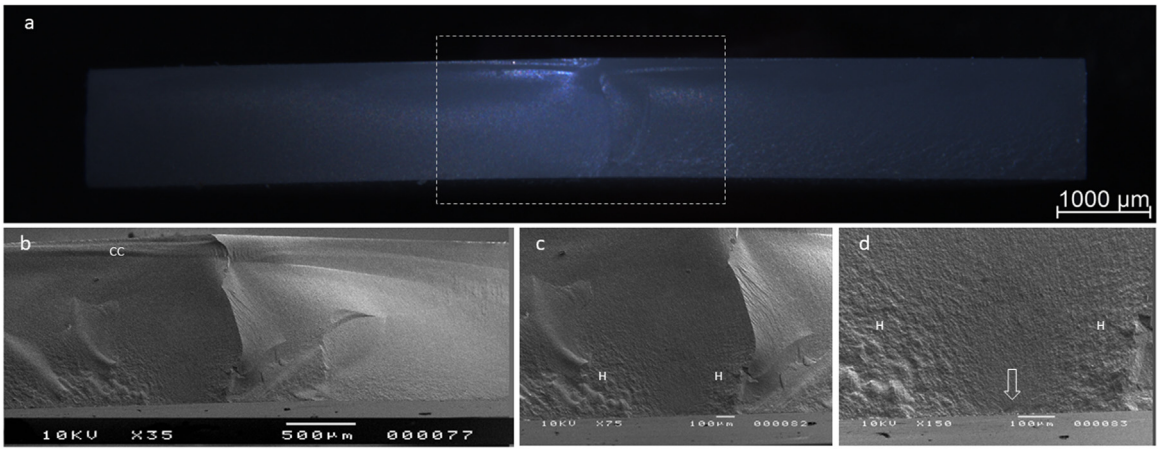

Fig. 5 – a) Stereomicroscopic image of the fractured surface of the ZTA Zpex 80/20 composite. b) SEM image of ZTA Zpex 80/20 fracture surface with 35× magnification. c) Indicators such as compression curl (CC), hackle lines (H) d) Area of fracture initiation (arrow) with 150x magnification.

Table 3 – Contrast ratio (CR) and translucency parameter (TP) mean values and corresponding 95% confidence interval of the studied groups.

Condition	Material	CR	TP
Immediate	Zpex	0.770 (0.010) ^{C}	10.214 (0.195) ^{B}
	ZTA Zpex 80/20	0.997 (0.007) ^{A}	0.186 (0.151) ^{D}
	Alumina	0.981 (0.007) ^{B}	2.384 (0.195) ^{C}
Aged	Zpex	0.657 (0.008) ^{D}	15.511 (0.374) ^{A}
	ZTA Zpex 80/20	0.998 (0.006) ^{A}	0.223 (0.290) ^{D}
	Alumina	0.979 (0.006) ^{B}	2.581 (0.374) ^{C}

Different letters mean statistical difference between groups.

preservation of the crystalline content with a slight increase in the amount of monoclinic zirconia after aging (2% increase), Zpex t-m phase transformation was notably higher after aging (26% increase). The ZTA composite stability may lie on the restrict interconnectivity of zirconia grains and higher hardness of the alumina, which limit the nucleation and growth process associated with phase transformation and LTD [33].

Some variability in biaxial flexural strength data has been reported among different commercially available dental Y-TZPs with values ranging from 817 MPa [34] to 1121 MPa [31], which is in agreement with the current findings. After aging in the oral environment for only 100 days, several zirconia ceramics already presented tetragonal-monoclinic phase transformation, changes in roughness and in flexural strength [35]. In the current study, ZTA Zpex 80/20 composite, despite the high percentage of alumina, showed biaxial flexural strength values within the range found in the literature for zirconia Y-TZP. The significant differences between ZTA Zpex 80/20 and aged Zpex may not influence the clinical indications of the experimental composite according to ISO 6872:2015 recommendations. From a strength's perspective only, both the polycrystalline composite and translucent zirconia ceramics may be indicated for partially or fully covered substructure of 4-unit or more FPDs (approximately 800 MPa) [36]. More work is warranted to further characterize the material and to match an appropriate porcelain veneer to corroborate these preliminary findings.

Concerning the influence of low-temperature degradation on the mechanical performance of materials, conflicting results are also found in the literature [37,38]. The current study demonstrated that aging did not affect the mechanical properties of the ZTA Zpex 80/20; on the other hand, the mechanical properties of the translucent zirconia were improved after aging (except for the Weibull modulus). This fact can be elucidated by the increase in the volume (~3–4%)

of zirconia grains during the t-m phase transformation and the consequent accumulation of compressive stress [39,40], as corroborated in the residual stress data. Therefore, it can be hypothesized that the volumetric increase of the grains was insufficient to reach the critical tension that would lead to the collapse of the grains, increase the population of defects in the material, and reduce the flexural strength [17]. A more aggressive aging protocol leading to higher percentages of t-m transformation would be necessary to reach the critical stress, which support future investigations. In contrast, the absence of residual stress and similar mechanical properties before and after aging suggest that the experimental ZTA composite presented hydrothermal stability and enhanced LTD resistance compared to Y-TZP translucent zirconia, as confirmed in the XRD and SEM analysis. Although ZTA composites have previously shown the resistance to LTD [25,28,41], there has been scarce information concerning the influence of aging on the mechanical performance of such composites that makes studies comparison a challenge.

Regarding the outcomes for optical properties, ZTA Zpex 80/20 composite showed lower translucency and higher masking ability relative to the translucent Y-TZP and alumina (irrespective of the aging condition), which may be associated with refractive index mismatch between the two phases and crystallography that hampers light transmission [42,43]. Such results recommend the application of the experimental composite as a FDP framework material, where porcelain veneering is needed for esthetic results, specially indicated where darkened substrates are present (colored endodontically treated teeth or titanium implant abutments). While the optical properties of the ZTA composite have not been altered by LTD, Zpex demonstrated a significant reduction in opacity values accompanied by a significant increase in translucency values after the aging protocol, which becomes a concern for the clinician, mainly when considering darkened substrates. A recent investigation revealed that the hydrothermal aging affected the optical properties of monolithic zirconia ceramics and its translucency increased with artificial aging [44]. It was also emphasized that certain color changes might be clinically apparent, and an esthetically improper difference may be expected about three to four years after cementation of the prostheses. The increased translucency may lie on crystalline content and microstructural alteration after aging, with t-m transformation initially leading to a defect and pore sealing that may favor light transmission, as depicted in the SEM micrographs [42,43].

It seems reasonable to highlight that the most extended randomized clinical trial (10 years follow-up) has shown statistically superior technical complication rates for porcelain fused to zirconia tooth-supported FDPs when compared to porcelain fused to metal FDPs. Those complications include framework fractures and significant fractures of the veneering ceramic [45]. Therefore, long-term outcomes of long-span zirconia prostheses still warrant more investigation, and current results encourage more investigations to promote the potential application of ZTA as a framework material for FDPs, as well as to investigate further innovations that can improve optical properties and potentially support its monolithic application.

5. Conclusion

The polycrystalline composite ZTA Zpex 80/20 presented a dense microstructure and homogeneous distribution of zirconia particles within the alumina matrix along with promising mechanical properties, which remained stable after artificial aging. Despite the stability, the optical properties of the composite indicated a low translucency and high opacity. Altogether, ZTA Zpex 80/20 properties encourage its use as a substructure for long span fixed dental prostheses, however further innovations should be endeavored to engineer ZTA with tooth-shaded appearance to optimize subsequent esthetic porcelain veneering or even to allow its monolithic application.

Acknowledgements

São Paulo Research Foundation (FAPESP) # 2012/19078-7, EMU 2016/18818-8; #2016/17793-1; #2017/19362-0; #2018/03072-6; #2019/08693-1, #2019/14798-0 # 2019/00452-5 and To Conselho Nacional de Desenvolvimento Científico e Tecnológico (CNPq), grant # 304589/2017-9; 434487/2018-0, and to Capes Financial Code 001.

REFERENCES

[1] Chevalier J, Gremillard L, Deville S. Low-temperature degradation of zirconia and implications for biomedical implants. Annu Rev Mater Res 2007;37:1–32.
[2] El-Ghany OSA, Sherief AH. Zirconia based ceramics, some clinical and biological aspects. Fut Dent J 2016;2:55–64.
[3] Hisbergues M, Vendeville S, Vendeville P. Zirconia: established facts and perspectives for a biomaterial in dental implantology. J Biomed Mater Res B Appl Biomater 2009;88:519–29.
[4] Denry I, Kelly JR. State of the art of zirconia for dental applications. Dent Mater 2008;24:299–307.
[5] Zhang J, Liao Y, Li W, Zhao Y, Zhang C. Microstructure and mechanical properties of glass-infiltrated Al_2O_3/ZrO_2 nanocomposites. J Mater Sci: Mater Med 2012;23:239–44.
[6] Chevalier J, Gremillard L, Virkar AV, Clarke DR. The tetragonal-monoclinic transformation in zirconia: lessons learned and future trends. J Am Ceram Soc 2009;92:1901–20.
[7] Jiang L, Liao Y, Wang C, Lu J, Zhang J. Low temperature degradation of alumina-toughened zirconia in artificial saliva. J Wuhan Univ Technol: Mater Sci Ed 2013;28:844–8.
[8] Tsubakino H, Nozato R, M Hamamoto. Effect of Alumina Addition on the Tetragonal-to-Monoclinic Phase Transformation in Zirconia–3 mol% Yttria. J Am Ceram Soc 1991;74:440–3.
[9] Ross I, Rainforth W, McComb D, Scott A, R Brydson. The role of trace additions of alumina to yttria–tetragonal zirconia polycrystals (Y–TZP). Scr Mater 2001;45:653–60.
[10] Kurtz SM, Kocagoz S, Arnholt C, Huet R, Ueno M, Walter WL. Advances in zirconia toughened alumina biomaterials for total joint replacement. J Mech Behav Biomed Mater 2014;31:107–16.
[11] Casellas D, Rafols I, Llanes L, Anglada M. Fracture toughness of zirconia–alumina composites. Int J Refract Metd Hard Mater 1999;17:11–20.
[12] Benalcazar Jalkh EB, Monteiro KN, Cesar PF, Genova LA, Bergamo ETP, Lopes ACO, et al. Aging resistant ZTA

composite for dental applications: microstructural, optical and mechanical characterization. Dent Mater 2020.
[13] Jalkh EB, Bergamo E, Monteiro K, Cesar P, Genova L, Lopes A, et al. Aging resistance of an experimental zirconia-toughened alumina composite for large span dental prostheses: optical and mechanical characterization. J Mech Behav Biomed Mater 2020;104:103659.
[14] Chevalier J, Cales B, Drouin JM. Low-temperature aging of Y-TZP ceramics. J Am Ceram Soc 1999;82:2150–4.
[15] Pereira G, Amaral M, Cesar PF, Bottino MC, Kleverlaan CJ, Valandro LF. Effect of low-temperature aging on the mechanical behavior of ground Y-TZP. J Mech Behav Biomed Mater 2015;45:183–92.
[16] Toraya H, Yoshimura M, S Somiya. Calibration curve for quantitative analysis of the monoclinic-tetragonal ZrO2 system by X-ray diffraction. J Am Ceram Soc 1984;67:C-119–221.
[17] Prado P, Monteiro JB, Campos TMB, Thim GP, de Melo RM. Degradation kinetics of high-translucency dental zirconias: mechanical properties and in-depth analysis of phase transformation. J Mech Beha Biomed Mater 2019;102:103482.
[18] Ceglias RB, Alves JM, Botelho RA, Baeta Júnior Ed S, Santos ICd, Moraes NRDCd, et al. Residual stress evaluation by X-ray diffraction and hole-drilling in an API 5L X70 steel pipe bent by hot induction. Mater Res 2016;19:1176–9.
[19] Guilardi LF, Pereira GKR, Wandscher VF, Rippe MP, Valandro LF. Mechanical behavior of yttria-stabilized tetragonal zirconia polycrystal: effects of different aging regimens. Braz Oral Res 2017;31:e94.
[20] Amaral M, Valandro LF, Bottino MA, Souza RO. Low-temperature degradation of a Y-TZP ceramic after surface treatments. J Biomed Mater Res B Appl Biomater 2013;101:1387–92.
[21] Pereira GKR, Muller C, Wandscher VF, Rippe MP, Kleverlaan CJ, Valandro LF. Comparison of different low-temperature aging protocols: its effects on the mechanical behavior of Y-TZP ceramics. J Mech Behav Biomed Mater 2016;60:324–30.
[22] Committee CT. Colorimetry. CIE Pub No 15.3. Vienna, Austria: CIE Central Bureau; 2004.
[23] Chevalier J. What future for zirconia as a biomaterial? Biomaterials 2006;27:535–43.
[24] Haraguchi K, Sugano N, Nishii T, Miki H, Oka K, Yoshikawa H. Phase transformation of a zirconia ceramic head after total hip arthroplasty. Bone Joint J 2001;83:996–1000.
[25] Deville S, Chevalier J, Fantozzi G, Bartolomé JF, Requena Jn, Moya JS, et al. Low-temperature ageing of zirconia-toughened alumina ceramics and its implication in biomedical implants. J Eur Ceram Soc 2003;23:2975–82.
[26] Pecharroman C, Bartolomé JF, Requena J, Moya JS, Deville S, Chevalier J, et al. Percolative mechanism of aging in zirconia-containing ceramics for medical applications. Adv Mater 2003;15:507–11.
[27] Ueno M. General Manager, Quality Assurance Corporate Division: Japan Medical Materials; 2012.
[28] Fabbri P, Piconi C, Burresi E, Magnani G, Mazzanti F, Mingazzini C. Lifetime estimation of a zirconia–alumina composite for biomedical applications. Dent Mater 2014;30:138–42.
[29] Tang DX, Lim HB, Lee KJ, Lee CH, Cho WS. Evaluation of mechanical reliability of zirconia-toughened alumina composites for dental implants. Ceram Int 2012;38:2429–36.
[30] Pereira GKR, Venturini AB, Silvestri T, Dapieve KS, Montagner AF, Soares FZM, et al. Low-temperature degradation of Y-TZP ceramics: a systematic review and meta-analysis. J Mech Behav Biomed Mater 2015;55:151–63.
[31] Nakamura K, Harada A, Ono M, Shibasaki H, Kanno T, Niwano Y, et al. Effect of low-temperature degradation on the mechanical and microstructural properties of tooth-colored 3Y-TZP ceramics. J Mech Behav Biomed Mater 2016;53:301–11.
[32] Pereira G, Silvestri T, Camargo R, Rippe M, Amaral M, Kleverlaan C, et al. Mechanical behavior of a Y-TZP ceramic for monolithic restorations: effect of grinding and low-temperature aging. Mater Sci Eng: C 2016;63:70–7.
[33] Chevalier J, Grandjean S, Kuntz M, Pezzotti G. On the kinetics and impact of tetragonal to monoclinic transformation in an alumina/zirconia composite for arthroplasty applications. Biomaterials 2009;30:5279–82.
[34] Ramos GF, Pereira GK, Amaral M, Valandro LF, Bottino MA. Effect of grinding and heat treatment on the mechanical behavior of zirconia ceramic. Braz Oral Res 2016;30.
[35] Borges MAP, Alves MR, dos Santos HES, dos Anjos MJ, Elias CN. Oral degradation of Y-TZP ceramics. Ceram Int 2019;45:9955–61.
[36] Standardization IOf. ISO 6872:2015—dentistry—ceramic materials; 2015.
[37] Flinn BD, deGroot DA, Mancl LA, Raigrodski AJ. Accelerated aging characteristics of three yttria-stabilized tetragonal zirconia polycrystalline dental materials. J Prosthet Dent 2012;108:223–30.
[38] Ban S, Sato H, Suehiro Y, Nakanishi H, Nawa M. Biaxial flexure strength and low temperature degradation of Ce-TZP/Al_2O_3 nanocomposite and Y-TZP as dental restoratives. J Biomed Mater Res B Appl Biomater 2008;87:492–8.
[39] Denry I, Kelly JR. Emerging ceramic-based materials for dentistry. J Dent Res 2014;93:1235–42.
[40] Nemli SK, Yilmaz H, Aydin C, Bal BT, Tiras T. Effect of fatigue on fracture toughness and phase transformation of Y-TZP ceramics by X-ray diffraction and Raman spectroscopy. J Biomed Mater Rest B Appl Biomater 2012;100:416–24.
[41] Perrichon A, Liu BH, Chevalier J, Gremillard L, Reynard B, Farizon F, et al. Ageing, shocks and wear mechanisms in ZTA and the long-term performance of hip joint materials. Materials 2017;10.
[42] Zhang Y. Making yttria-stabilized tetragonal zirconia translucent. Dent Mater 2014;30:1195–203.
[43] Walczak K, Meissner H, Range U, Sakkas A, Boening K, Wieckiewicz M, et al. Translucency of zirconia ceramics before and after artificial aging. J Prosthodont 2019;28:e319–24.
[44] Kim HK, Kim SH. Effect of hydrothermal aging on the optical properties of precolored dental monolithic zirconia ceramics. J Prosthet Dent 2018.
[45] Sailer I, Balmer M, Husler J, Hammerle CHF, Kanel S, Thoma DS. 10-year randomized trial (RCT) of zirconia-ceramic and metal-ceramic fixed dental prostheses. J Dent 2018.